Image Statistic Models Characterize Well Log Image Quality

Somdyuti Paul and Alan C. Bovik, *Fellow, IEEE*

***Abstract*—Assessing the image quality of well logs is essential to ensure the accuracy of their digitization and subsequent processing. Currently, the suitability of well logs for information retrieval is solely determined on the basis of subjective judgments of their image quality by human experts. The success of Natural Scene Statistics (NSS) based models that are used to conduct no reference quality assessment of photographic images motivates us to try to exploit them to characterize the quality of non-photographic images such as well logs. Accordingly, we develop a scheme to characterize the quality of a well log as 'acceptable' or 'unacceptable' for subsequent processing based on the Natural Image Quality Evaluator (NIQE), a successful no reference image quality assessment model based on natural scene statistics. Our experimental results show that the objective quality scores thus obtained can be reliably used to eliminate well logs of inferior quality from the processing pipeline, which can serve as a beneficial step to reduce the human hours spent in examining well logs and to improve the rate of information retrieval as well as the accuracy of retrieved information. Source code for the trained well log image quality predictor is available at https://github.com/Somdyuti2/Well_log_IQA.**

***Index Terms*—Natural scene statistics, image quality assessment, natural image quality evaluator, well logs.**

I. Introduction

THE technique of well logging is used in the oil and natural gas industry to measure the geological properties of formations in oil and gas wells. The data thus obtained, known as a well log, is recorded as a continuous function of the formation's depth and is represented in a graphical form. Diverse data, including thickness of a formation, porosity, water saturation, temperature, presence of oil and natural gas, resistivity, reservoir pressure etc. can be collected and recorded in the form of well logs, which are stored as printed records or in an electronic format. Often, well logs are subjected to a digitization process before they are analyzed to produce useful data for purposes such as assessing the viability of a well or to improve its efficiency.

Software used for digitizing well logs typically require human intervention, chiefly to guide the curve tracing. This is a critical step, the precision of which is largely dependent on the perceptual visual quality of the well logs, which affects their intelligibility to humans. A sharp well log curve is easily traceable, whereas smudged or faint ones are hard to trace; sometimes, a well log image might have large regions of obfuscated or missing curves rendering them untraceable, and thus useless. The amount of human intervention, and thereby the time required for digitization could be significantly reduced if such untraceable well logs were automatically identified and eliminated beforehand. Here, we develop such a screening approach, by adapting a successful no refernce (NR) picture quality predictor [1] to assess scanned well logs images towards characterizing whether a well log meets a minimum perceptual quality standard to allow for successful information retrieval.

The standard tools for developing picture quality models and algorithms are databases of exemplar distorted pictures along with large number of human subjective annotations of them. However, as compared to ordinary photographic images of the world around us, it is substantially more difficult to acquire subjective ratings on well logs for two reasons. First of all, unlike photographic images, rating well logs require domain specific knowledge to recognize the distortions that degrade its information content; secondly, the dimensions of well log images are much larger than even the largest resolution photographic images encountered in practice. As such an entire well log cannot be displayed at once and must be scrolled for examination. Further, the quality of a well log is likely to vary as it is scrolled. A single severely distorted patch may render the entire well log useless. Since it is onerous to peruse a well log of order $10^3 \times 10^6$ pixels, a scheme for effectively combining the scores assigned to different segments also needs to be devised. In light of the above facts, the principal contribution presented in this letter is to adapt a perceptually relevant statistical image model to derive quality-sensitive features that are combined to predict well log image quality without the need for any subjective ratings, i.e. in a generic training free manner.

II. Related Work

The perceptual visual quality of images and videos of natural scenes is relevant to a multitude of applications, including analysing the performance of compression standards, monitoring consumer video streams, optimizing algorithms for image restoration, enhancement, denoising etc. As a result, objective Image Quality Assessment (IQA) has received consistent attention from researchers, leading to the development of widely adopted techniques such as the Structural Similarity Index (SSIM) [2]. In addition to images of natural scenes, i.e. standard optical photographic images of the world, there exists a wide variety of scientific imagery such as hyperspectral images (HSI) and Synthetic aperture radar (SAR) images for remote sensing applications, Magnetic Resonance Imaging

Manuscript received September 11, 2018; revised November 22, 2018 and January 03, 2019; accepted January 10, 2019.

The authors are with the Department of Electrical and Computer Engineering, University of Texas at Austin, Austin, TX, 78712, USA (e-mail: somdyuti@utexas.edu; bovik@ece.utexas.edu).

(MRI), Computed Tomography (CT) and ultrasound images for medical applications, and many others. Since these kinds of scientific data are often analyzed and processed by computers in addition to being examined by human experts, it is reasonable to assume that the results of any such analysis would be sensitive to the quality of the images being used. However different kinds of scientific imagery are governed by different statistics and distortion models; thus it is plausible that successful IQA techniques for photographic images, especially those that are distortion specific, may not be amenable to IQA of any particular type of scientific images. Thus specialized application oriented IQA techniques have been proposed for scientific imagery. For example, given an undistorted version of the image whose quality is to be evaluated as reference, the Full Reference IQA (FR IQA) SSIM algorithm has been adapted to evaluate the quality of SAR images [3] and medical images [4].

In many applications however, an undistorted version of the image being evaluated is not available. In such instances, NR IQA techniques are applicable and popular ones such as [1], [5], [6] which rely on various NSS models are usually used. In such cases, the perceptual quality of a given image is predicted by measuring its deviation from a model of image statistics. A similar paradigm using statistical model features derived under models of pristine and distorted images was shown to work well for certain non-photographic images such as HSI [7] and structural MRI [8].

Here, we develop a general way to evaluate the quality of scanned well log images without assuming the benefit of associated undistorted reference images or of subjective quality scores on exemplar distorted well log image data. To the best of our knowledge, there has been no prior work on quality assessment of this particular type of scientific image. In the subsequent sections of this letter, we show that the statistics of scanned well logs are adequately characterized under the statistical model that is used to define the Natural Image Quality Evaluator (NIQE) [1], which is a NR IQA scheme based on a certain NSS model. The modeled statistics can thenceforth be used to characterize well logs as 'acceptable' or 'unacceptable.'

III. Proposed Method

In this section we describe the NR IQA technique that we have developed for scanned well logs based on NSS. The fact that the NIQE model of [1] does not require subjective scores for training makes it well suited to the present problem of assessing the perceptual quality of well log images without training on any associated subjective scores.

A. Datasets

We performed our experiments on two well log image datasets as described below:

Dataset A: This dataset comprises large set of scanned well logs of varying perceptual qualities. The images were provided by Drillinginfo and subjectively classified into two broad categories - 'acceptable' and 'unacceptable,' by three experts experienced in the well log digitization process and thus familiar with the distortions affecting information retrieval. The dataset has 193 well logs labeled as 'acceptable' and 36 as 'unacceptable'. A skewed distribution is expected since only a few of the scanned images were degraded to the extent of being rated as unfit for further processing. Further, more images from the 'acceptable' category are desirable since they are used to model the statistics of acceptable well logs. Accordingly, our training set comprises 157 'acceptable' well log images from dataset A. The remaining 72 well logs images (36 in each category) are utilized for testing the performance of the model.

Dataset B: We collected a set of publicly available scanned well-logs from diverse sources[1] to create this dataset. It consists of 64 images each from the 'acceptable' and 'unacceptable' categories. Equal number of images were purposely chosen from each category since this dataset was designed to be used to evaluate the model's performance.

The 'acceptable' category includes well log images having manually traceable curves, readable axis labels and mostly sharp grid lines; these characteristics allow well logs to be accurately digitized and thereby analyzed further to extract useful information. On the other hand, the 'unacceptable' category comprises well logs having large regions of faint, missing or smudged curves and grid lines, and/or illegible axis labels. Since the values of illegible axis labels and curve points at the missing or obscured segments can only be surmised, the presence of such distortions can lead to digitization of a well log image that is unfit for practical use. We have made use of such characteristics of 'acceptable' and 'unacceptable' well-log images as guidelines for assigning the subjective labels to the images from dataset B. The visual characteristics of the 'acceptable' and 'unacceptable' well logs described above are illustrated by a segment of an example well log from each category in Figure 1.

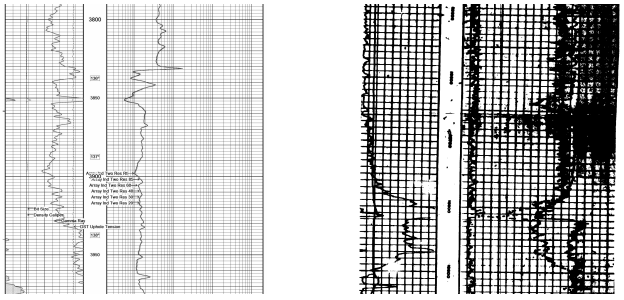

(a) Acceptable (b) Unacceptable

Fig. 1. Examples of acceptable and unacceptable well logs.

B. Preprocessing

The scanned well logs consists of grayscale as well as color images. We converted all images to grayscale prior to further processing. The resolutions of the scanned well logs are typically of the order of $10^3 \times 10^6$ pixels, which is far larger than resolutions commonly used for rendering

[1]Dataset B is sourced from http://www.wvgs.wvnet.edu/www/tbr/TBR_well_logs.asp and from https://rrcsearch3.neubus.com/esd3-rrc/index.php?_module_=esd&_action_=keysearch&profile=15

photographic images. To train the NIQE model, each image was split into blocks of size 512×512 for computational ease. A given 512×512 block is denoted as I, and a local divisive normalization at every pixel coordinate (i, j) is performed which serves to decorrelate the brightness values of neighboring pixels. We thus obtain the mean subtracted contrast normalized (MSCN) coefficients:

$$\hat{I}(i,j) = \frac{I(i,j) - \mu(i,j)}{\sigma(i,j) + 1}, \tag{1}$$

where the local mean $\mu(i, j)$ and standard deviation $\sigma(i, j)$ are given by:

$$\mu(i,j) = \sum_{k=-K}^{K} \sum_{l=-L}^{L} w_{k,l} I(i+k, j+l) \tag{2}$$

$$\sigma(i,j) = \sqrt{\sum_{k=-K}^{K} \sum_{l=-L}^{L} w_{k,l} [I(i+k, j+l) - \mu(i,j)]^2} \tag{3}$$

where w is a 2D circularly symmetric unit volume Gaussian weighting function sampled out to three standard deviations, where $K = L = 3$.

C. NIQE Model Fitting

In order to analyze the local statistics of the MSCN and paired product coefficients, square patches of size $P \times P$ are selected whose patch standard deviations (3) lie above a threshold τ [1]. The distributions of the MSCN and paired product coefficients are then modeled on each patch. For photographic pristine images, the MSCN coefficients as derived in equation 1 generally adhere to a Gaussian distribution, as has been shown in many prior studies [9]–[11]. This distribution is violated in the presence of perceptual distortions of photographic images, and also for non-photographic images such as well logs. In general, the MSCN distribution can be modeled by a Generalized Gaussian Distribution (GGD) [6]:

$$f(x; \alpha, \sigma^2) = \frac{\alpha}{2\beta\Gamma(\frac{1}{\alpha})} \exp\left(- \left(\frac{|x|}{\beta} \right)^{\alpha} \right) \tag{4}$$

where $\beta = \sigma \sqrt{\frac{\Gamma(\frac{1}{\alpha})}{\Gamma(\frac{3}{\alpha})}}$ and $\Gamma()$ is the gamma function.

Further, it has been shown in [6] that distortion information can be captured by modeling the distributions of the products of adjacent MSCN coefficient pairs in the horizontal, vertical and the two diagonal directions. The distributions of the MSCN products are well modeled as following an Asymmetric Generalized Gaussian Distribution (AGGD) whose functional form is given by:

$$f(x; \nu, \beta_l^2, \beta_r^2) = \begin{cases} \frac{\nu}{(\beta_l + \beta_r)\Gamma(\frac{1}{\nu})} \exp\left(- \left(\frac{(-x)}{\beta_l} \right)^{\nu} \right) & \forall x \leq 0 \\ \frac{\nu}{(\beta_l + \beta_r)\Gamma(\frac{1}{\nu})} \exp\left(- \left(\frac{(x)}{\beta_r} \right)^{\nu} \right) & \forall x \geq 0 \end{cases} \tag{5}$$

The mean of the AGGD is given by:

$$\eta = (\beta_r - \beta_l) \frac{\Gamma(\frac{2}{\nu})}{\Gamma(\frac{1}{\nu})} \tag{6}$$

Each AGGD is completely described by four parameters, $(\beta_l, \beta_r, \nu, \eta)$. These four parameters as well as the two parameters of the GGD, α and σ^2 can be efficiently estimated by the moment matching approach [6], and serves as key features in our model.

Figure 2 illustrates the MSCN and paired product MSCN distributions for the example segments of 'acceptable' and 'unacceptable' well logs from Figure 1. In order to highlight the differences between the MSCN statistics of well logs and photographic images, we also show the corresponding distributions of a photographic pristine image from the LIVE IQA database [12] and its distorted version corrupted with additive white Gaussian noise of mean zero and variance 0.2. From the figure, it is clear that instead of the smooth distribution we obtain for photographic images, the well log MSCN distribution is characterized by sharp peaks, indicating dominance of a few gray levels. The well logs having the best perceptual quality typically have a saturated appearance with a large number of pixels being white or almost white, with sharp dark scribbles and gridlines running across the length; since the bright pixels outnumber the dark pixels, the normalized distribution is also slightly skewed to the right. As distortions are introduced by the scanning process, the scribbles and grids become smudged leading to more dark pixels, thereby reducing the rightward skew. Similar differences in the characteristic of product MSCN coefficients is observed. From Figure 2 it is evident that not only do the scene statistics vastly differ for well logs and photographic images, but also the differences between pristine and distorted distributions are more subtle on well log images. The implication is that the general NIQE model that has been trained on pristine photographic images and made publicly available would not adequately capture the statistics of well logs. Thus, we require dedicated modeling in this case. Accordingly, we use the parameters of the distribution obtained from the selected patches of the 'acceptable' well logs from the training set to construct the IQA model. By modeling the products of MSCN coefficients along the same 4 directions with AGGD models, each defined by 4 parameters, we obtain a total of 16 parameters. These 16 parameters along with the 2 parameters (α, σ) of the GGD model fit of the MSCN coefficients yields a total of 18 parameters at the original scale of the image. The same parameters are also computed at a lower scale of resolution by low-pass filtering followed by downsampling by a factor of 2. Thus a 36 dimensional feature $\mathbf{x}$ is obtained from each patch of the 'acceptable' well logs. A Multivariate Gaussian (MVG) model is used to fit the distribution of this NSS feature $\mathbf{x}$ across all selected patches in the training data:

$$f(\mathbf{x}) = \frac{1}{(2\pi)^{k/2} |\Sigma|^{1/2}} \exp(-\frac{1}{2} (\mathbf{x} - \nu)^T |\Sigma|^{-1} (\mathbf{x} - \nu)) \tag{7}$$

The mean ν and the covariance Σ of the MVG model are estimated by standard maximum likelihood estimation.

D. No Reference Quality Assessment

The 36 dimensional feature vector as described above is computed on each patch of the well log whose quality is to be evaluated; the sharpness criterion is not applied to the

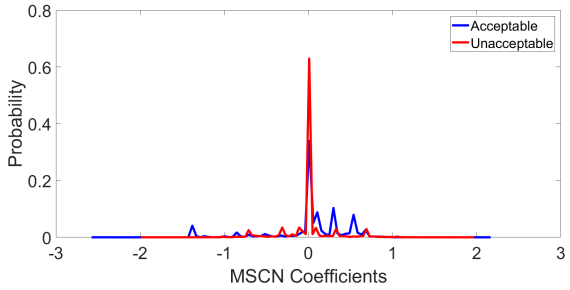

(a) Histogram of MSCN coefficients of well log images.

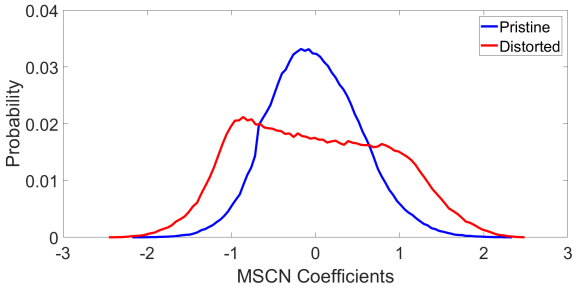

(b) Histogram of MSCN coefficients of a photographic image

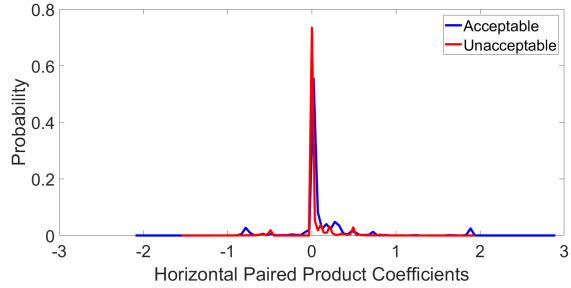

(c) Histogram of products of adjacent MSCN coefficients of well log images.

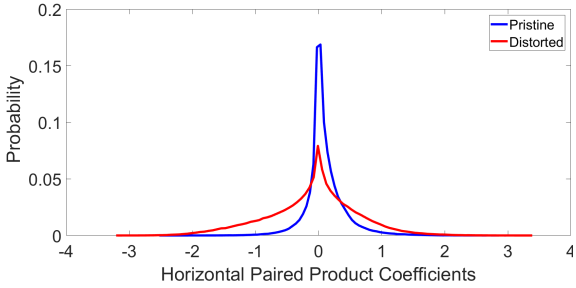

(d) Histogram of products of adjacent MSCN coefficients of a photographic image.

Fig. 2. Empirical distributions of MSCN and products of adjacent MSCN coefficients.

test patches, since loss of sharpness is inherently related to the loss of quality. This is followed by multivariate Gaussian fitting (7). The NIQE index is then computed as the distance between the parameters of the MVG fit obtained from the patches of acceptable well logs and those from the test well log as follows:

$$D(\nu, \nu_{test}, \Sigma, \Sigma_{test}) = \sqrt{(\nu - \nu_{test})^T \frac{\Sigma + \Sigma_{test}}{2} (\nu - \nu_{test})} \quad (8)$$

here ν and Σ are the MVG parameters of the 'acceptable' well log model while ν_{test} and Σ_{test} are the corresponding parameters obtained from the test well log. Since the quality score is computed as a distance between features derived from 'acceptable' and 'unacceptable' well log statistics, lower scores correspond to better quality.

IV. Experimental Results

In our experiments, we use patches with $P = 96$ to calculate the MSCN and MSCN product coefficient distributions. The sharpness threshold τ was chosen to be 0.75 of the peak patch sharpness as defined in [1]. The trained model was tested on a set of 36 well logs each from the 'acceptable' and 'unacceptable' categories of dataset A, and on 64 well logs from each of the two categories on dataset B. The difference in visual quality between 'acceptable' and 'unacceptable' well logs was found to strongly correlate with their corresponding distance scores. This is illustrated in Figure 3 by the distribution of the scores. The 'acceptable' well logs were found to have much lower scores as compared to the 'unacceptable' ones, as desired on both the datasets. Figure 3 also shows the corresponding distance score distributions obtained using the NIQE model for photographic images; in this case, the scores from the 'acceptable' and 'unacceptable' category are found to overlap significantly. This indicates that standard no reference image quality assessment techniques intended for photographic, naturalistic images like NIQE, are less suited for analyzing the quality of well logs images. For further clarity, the relevant measures of variation of the distance scores obtained by our method are presented in Table I.

In order to demarcate 'acceptable' well log images from 'unacceptable' ones, the quality scores should be thresholded such that the empirical 'acceptable' and 'unacceptable' score distributions are placed as far apart from the threshold as possible. However, since the variance of the 'acceptable' category is considerably larger, it is reasonable to allow a larger margin of separation from the threshold for the 'acceptable' score distribution. Setting the threshold close to 6.0 allows a large margin of separation for 'acceptable' and a smaller margin for 'unacceptable'. Thus, a test well log image is classified as 'acceptable' if it is scored below the threshold by our model and vice versa. Using a threshold of 6.0 and treating the acceptable well logs as positives, the accuracy, precision and recall metrics obtained using our model on both the datasets are summarized in the Table II. Although the same threshold achieves good performance on both the datasets as demonstrated by Table II, we do not suggest designating a hard threshold for performing generic segregation of well logs, since the quality of a well log which is deemed acceptable may depend on the use case and we do not claim that our results are comprehensive over the field. Still, the achieved category separation is compelling. At this point, the model may be tuned on a per use case basis to achieve best performance. For instance, for an use case involving a larger number of a certain type of well log images a small subset of data can be used

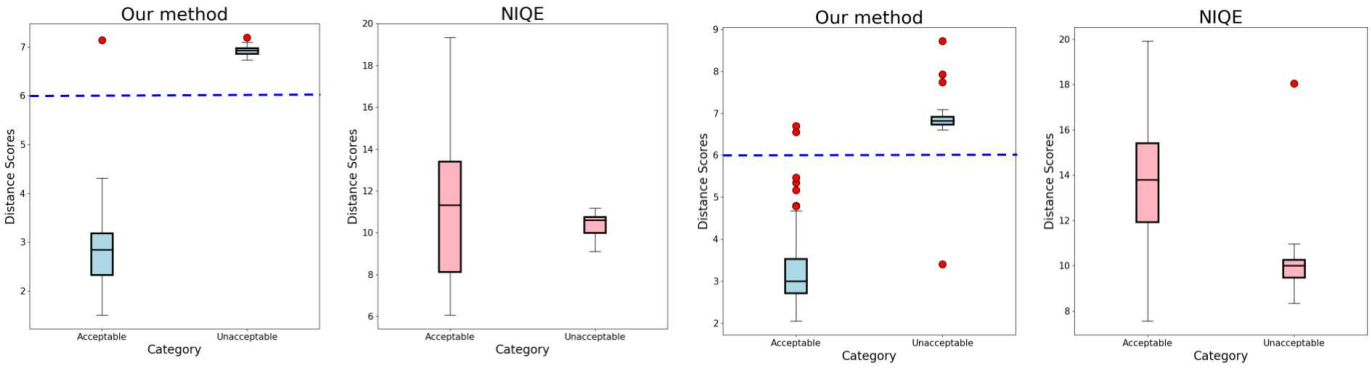

(a) Dataset A (b) Dataset B

Fig. 3. Distribution of scores of test well logs with box plots, with threshold shown as a dashed line.

TABLE I
MEASURES OF VARIATION OF QUALITY SCORES

Dataset	A		B	
	Acceptable	Unacceptable	Acceptable	Unacceptable
Mean	2.8768	6.9147	3.32	6.832
Variance	0.9220	0.0132	0.9162	0.2853

to tune the threshold to achieve maximum margin separation between the two category score distributions on that subset. Subsequently, the threshold thus tuned can be used to classify all well log images encountered in that use case.

TABLE II
PERFORMANCE METRICS OF THE TRAINED MODEL.

Dataset	Accuracy (%)	Precision (%)	Recall (%)
A	98.61	100	97.22
B	97.66	98.41	96.88

V. CONCLUSION

In this letter, we demonstrated that a natural image statistic model can be employed to categorize scanned well log image quality, allowing us to effectively identify and eliminate well logs of quality unfit for an accurate digitization. Although the NSS model employed in this letter was originally designed for photographic images whose statistics markedly differ from those of well logs, a significant revelation is that the NSS model is versatile enough to capture and differentiate well log image statistics. In principle, the objective IQA metrics thus obtained can be used to order a given database of well logs from best to worst perceptual quality; such an ordering would enable users to inspect, digitize or process the well logs in order of their decreasing quality thereby increasing efficiency and throughput. However, in the absence of subjective quality scores on the well logs, correspondences between the derived quality metrics and granular perceptual quality ratings cannot yet be established. Acquiring such subjective ratings to conclusively establish the performance of our model for ordering well logs according to their quality is a future direction that we plan to pursue.

ACKNOWLEDGMENT

The authors would like to thank Mark Lai, Justin Smith and Brian Umlang from DrillingInfo for providing the data which has been used to develop the model and for informative discussions on the practical factors which determine a well log's quality and usefulness. This research was supported by a grant from Drillinginfo.

REFERENCES

[1] A. Mittal, R. Soundararajan, and A. Bovik, "Making a completely blind image quality analyzer," *IEEE Signal Processing Letters*, vol. 20, no. 3, pp. 209–212, 2013.

[2] Z. Wang, A. C. Bovik, H. R. Sheikh, and E. P. Simoncelli, "Image quality assessment: from error visibility to structural similarity," *IEEE transactions on image processing*, vol. 13, no. 4, pp. 600–612, 2004.

[3] S. Jiao and W. Dong, "SAR image quality assessment based on SSIM using textural feature," in *Image and Graphics (ICIG), 2013 Seventh International Conference on*. IEEE, 2013, pp. 281–286.

[4] Y. Hua, L. Liu, and Q. Zhao, "Medical image quality assessment via contrast masking," in *Image and Signal Processing (CISP), 2015 8th International Congress on*. IEEE, 2015, pp. 964–968.

[5] M. A. Saad, A. C. Bovik, and C. Charrier, "Blind image quality assessment: A natural scene statistics approach in the DCT domain," *IEEE transactions on Image Processing*, vol. 21, no. 8, pp. 3339–3352, 2012.

[6] A. Mittal, A. Moorthy, and A. Bovik, "No-reference image quality assessment in the spatial domain," *IEEE Transactions on Image Processing*, vol. 21, no. 12, pp. 4695–4708, 2012.

[7] J. Yang, Y. Zhao, C. Yi, and J. C.-W. Chan, "No-reference hyperspectral image quality assessment via quality-sensitive features learning," *Remote Sensing*, vol. 9, no. 4, p. 305, 2017.

[8] J. P. Woodard and M. P. Carley-Spencer, "No-reference image quality metrics for structural MRI," *Neuroinformatics*, vol. 4, no. 3, pp. 243–262, 2006.

[9] D. L. Ruderman, "The statistics of natural images," *Network: computation in neural systems*, vol. 5, no. 4, pp. 517–548, 1994.

[10] M. J. Wainwright and E. P. Simoncelli, "Scale mixtures of gaussians and the statistics of natural images," in *Advances in neural information processing systems*, 2000, pp. 855–861.

[11] H. R. Sheikh and A. C. Bovik, "Image information and visual quality," in *Acoustics, Speech, and Signal Processing, 2004. Proceedings.(ICASSP'04). IEEE International Conference on*, vol. 3. IEEE, 2004, pp. iii–709.

[12] H. R. Sheikh, M. F. Sabir, and A. C. Bovik, "A statistical evaluation of recent full reference image quality assessment algorithms," *IEEE Transactions on image processing*, vol. 15, no. 11, pp. 3440–3451, 2006.